An analysis of cerebral blood flow from middle cerebral arteries during cognitive tasks via functional transcranial Doppler recordings

Meng Li[a], Hanrui Huang[a], Michael L. Boninger[b], Ervin Sejdić[a,*]

[a] *Department of Electrical and Computer Engineering, Swanson School of Engineering, University of Pittsburgh, Pittsburgh, PA, 15261, USA*
[b] *Department of Physical Medicine and Rehabilitation, University of Pittsburgh, Pittsburgh, PA, 15261, USA*

Abstract

Functional transcranial Doppler (fTCD) is a useful medical imaging technique to monitor cerebral blood flow velocity (CBFV) in major cerebral arteries. In this paper, CBFV changes in the right and left middle cerebral arteries (MCA) caused by cognitive tasks, such as word generation tasks and mental rotation tasks, were examined using fTCD. CBFV recordings were collected from 20 healthy subjects (10 females, 10 males). We obtained both the raw CBFV signal and the envelope CBFV signal, which is the maximal velocity to gain more information about the changes and hemisphere lateralization in cognitive tasks compared to the resting state. Time, frequency, time-frequency, and information-theoretic features were calculated and compared. Sex effects were also taken into consideration. The results of our analysis demonstrated that the raw CBFV signal contained more descriptive

*Ervin Sejdić is the corresponding author.
Mailing address: Department of Electrical and Computer Engineering, Swanson School of Engineering, University of Pittsburgh, Pittsburgh, PA, 15261, USA.
Tel: +1-412-624-0508. E-mail: esejdic@ieee.org

information than the envelope signals. Furthermore, both types of cognitive tasks produced higher values in most signal features. Geometric tasks were more distinguished from the rest-state than verbal tasks and the lateralization was exhibited in right MCA during geometric tasks. Our results show that the raw CBFV signals provided valuable information when studying the effects of cognitive tasks and lateralization in the MCA.
Keywords: functional transcranial Doppler, cognitive tasks, rest, cerebral blood flow velocity, signal characteristics.

---

1. Introduction

The transcranial Doppler sonography (TCD) was first introduced by Aaslid in 1982, who utilized the TCD to measure the blood flow velocity in large basal arteries (Aaslid et al., 1982). TCD is useful for investigating mental activities because of the closely coupled relationship betwen mental activities and cerebral metabolism (Paulson et al., 2009). The diameter of the large basal arteries, including middle cerebral, anterior cerebral, and posterior cerebral arteries, is assumed to be fixed, so changes in brain perfusion results in velocity changes (Huber and Handa, 1967). Due to the frequency dependence on ultrasonic wave attenuation, researchers use a relatively low ultrasonic frequency (2MHz) and the thinnest part of the skull (transtemporal window) for insonation (the exposure to ultrasound) (White and Venkatesh, 2006). Compared with other neuroimaging techniques, such as positron emission tomography and functional magnetic resonance imaging, TCD is known for its high temporal resolution, and its ability to continuously measure blood flow velocity in a variety of conditions (Duschek and

Schandry, 2003).

Because MCAs supply much of the brain area involved in cognitive processing tasks, almost all of the studies investigating cognitive functions insonate MCAs (Ingvar and Risberg, 1965), (Risberg and Ingvar, 1973), (Lassen et al., 1978), (Risberg, 1986). Bilateral insonation is often used to measure cerebral blood flow velocity (CBFV) (e.g., (Deppe et al., 2000), (Knecht et al., 1998a), (Knecht et al., 1998b), (Schmidt et al., 1999)) but the reliability of detection of CBFV using bilateral insonation varies across different cognitive tasks (Knecht et al., 1998a). There is evidence showing that the CBFV during mental activities was more rapid than that during baseline periods (e.g. (Droste et al., 1989b), (Kelley et al., 1992)). The effects of tasks on lateralization has been studied by previous researchers; for example, Markusand and Boland showed a left-sided increase for right-handed participants in a word association task (Markus and Boland, 1992). Similar results were observed in other studies (e.g., (Tiecks et al., 1998), (Hartje et al., 1994)). The results were more equivocal for tasks involving spatial processing (e.g., mentally rotating shapes). A greater increase in CBFV was observed in the right MCA (Klingelhöfer et al., 1994), (Klingelhöfer et al., 1997), but the result of R-MCA dominance within spatial processing was not verified (e.g., (Hartje et al., 1994), (Gur and Reivich, 1980)). TCD studies also have shown that females have higher velocities than males at the same ages (e.g., (Russo et al., 1986), (Vriens et al., 1989)).

Previous work (e.g., (Duschek and Schandry, 2003), (Matteis et al., 2009)) has focused only on the envelope signals (i.e. peak velocities) and thus possibly lack the information only embodied in raw signals (Deppe et al., 2004).

A recent study showed that the raw CBFV signals contain significantly different characteristics in the resting state (Sejdić et al., 2013). Therefore, we focused on raw and enveloped CBFV signals in the current study in order to understand the MCA blood flow change caused by language and spatial tasks, as well as the lateralization associated with these cognitive tasks. Furthermore, we used information-theoretic approaches and time-frequency techniques that have not been previously incorporated into the study of cognitive tasks effects on CBFV signals. We analyzed both the envelope and the raw CBFV signals with focus on information found in the higher frequency content of raw CBFV signals and the effects of cognitive tasks on the features extracted from the raw CBFV signals. Considering additional information sources and a comprehensive list of features can enable us to understand finer clinical differences.

2. Methodology

2.1. Subjects

Twenty healthy participants (10 females, 10 males; 21.5 ± 1.86 years old; 67.9±14.2 kg; 174±9.69 cm) participated in the experiment. Before each data collection session, participants signed consent forms that were approved by the University of Pittsburgh Institutional Review Board. Then, participants filled out basic information forms, screening questionnaires, and Edinburgh handedness tests (Oldfield, 1971). No participants were found to have a history of concussions, heart murmurs, strokes, migraines, or other neurological conditions or brain-related injuries. Among these twenty participants, 16 subjects were right-handed with a mean score of 64% (38-93%), 3 subjects

were left-handed with a mean score of 80% (76-88%) and one was determined as ambidextrous.

2.2. Procedure

Participants were initially seated in front of a computer monitor. The investigator informed them about the importance and the goal of this study. In this experiment, we insonated MCAs by using a SONORA TCD system (CareFusion, San Diego, CA, USA). One 2MHz transducer was stabilized to the left-side transtemporal window, and another 2MHz transducer was stabilized to the right-side transtemporal window. The transtemporal window is located approximately above the zygomatic arch (Alexandrov et al., 2007). The TCD's depth was initialized to 50mm to approximate the mid-point of the MCA segment depth (Monsein et al., 1995). A plastic headband was used to adjust and fix the positions of the two probes. The insonation angle was then optimized by manually rotating the incident angle and following the sound and velocity of insonation. Once the TCD transducers were aptly positioned and fixed, the nasal cannula was placed under the nose to detect the end-tidal CO_2 ($ETCO_2$) levels which might affect CBFV in the MCA (Markwalder et al., 1984). The $ETCO_2$ levels were measured using a Capnocheck Sleep Capnograph/Oximeter (Smiths Medical, Dublin, OH, USA). Figure 1 depicts the experimental setup.

The experiment consisted of three parts. In the first part, the participants rested for 20 minutes which provided us with baseline information (Sejdić et al., 2013). The next two parts consisted of two 15-minute periods involving cognitive tasks, with a 5-minute break between each 15-minute period. Each 15-minute period consisted of five mental rotation tasks, five

word generation tasks in random order and 45-second resting periods between each task. These tasks were presented as visuospatial stimuli on a computer screen because it is expected that a visual mode of presentation does not influence the expected significant CBFV changes of the linguistic tasks (Stroobant and Vingerhoets, 2000).

2.2.1. Mental rotation task

Pairs of images, randomly selected from a database of shapes constructed from 3-D cubes (Peters and Battista, 2008) (see Figure 2), were displayed for 9 seconds each during the 45-second activation periods of tasks. In each pair of images, the patterns were either identical or mirror symmetrical. Participants were asked to determine whether the image pairs were identical or symmetric by mentally rotating the patterns.

2.2.2. Word generation task

An arbitrarily chosen capital letter was displayed on the screen during the activation periods. During this period, we instructed the participants to use nonverbal modes of responding, i.e. to think of words starting with that letter. A nonverbal mode was used to avoid any artifacts from speech or changes in intrathoracic pressure (Diehl et al., 1990), (Silvestrini et al., 1994).

2.2.3. Resting state

During the resting state, subjects were instructed to remain awake, relax and maintain a thought-free mental state.

3. Feature extraction

Here, we summarize a comprehensive set of features to be used in the analysis of recorded signals. The features were chosen in order to gain a detailed understanding of cerebral blood flow characteristics in time, frequency, and time-frequency domains. This is an essentially critical step if cerebral blood flow signals are to be used in other applications such as brain-machine interfaces (e.g., (Myrden et al., 2011), (Myrden et al., 2012)) or in order to understand brain laterilazation during cognitive tasks (e.g., (Hartje et al., 1994), (Gur and Reivich, 1980)). The considered features are often utilized in other biomedical applications (e.g., (Aboy et al., 2006), (Porta et al., 2001), (Sejdić et al., 2010)) and provide comprehensive descriptions of signal characteristics. Such detailed descriptions enable us to understand finer differences among rests, verbal tasks, and geometric tasks considered in this manuscript. Considering only traditional characteristics such as mean or variance is not necessarily sufficient to understand clinical/pathological differences.

3.1. Statistical features

The second, third, and forth moments of the signals were considered as we calculated standard deviation, skewness, and kurtosis (Papoulis, 1991). The cross-correlation at zero lag is also considered in this study to demonstrate whether left and right channels are related (Papoulis, 1991).

3.2. Information-theoretic features

The Lempel-Ziv complexity (LZC) has been widely used in biomedical applications to measure the randomness in a finite sequence (Aboy et al., 2006). The signal has to be first transformed to a finite sequence, $c(n)$,

denoting the number of sequence blocks in the concatenation. The LZC can be calculated as follows:

$$LZC = \frac{c(n)[\log_{100} c(n) + 1]}{n} \tag{1}$$

where the logarithmic base of 100 indicated the signal was quantized to 100 levels. When n is very large, $c(n) \leq \frac{n}{\log_{100} n}$ (Lempel and Ziv, 1976),(Cover and Thomas, 2006), thus the equation above can be simplified as

$$LZC = \frac{c(n) \log_{100} n}{n} \tag{2}$$

The entropy rate measures the unpredictability or the uncertainty of a signal (Porta et al., 2001). To calculate the entropy rate, the signal is first normalized and quantized to 10 equal levels. The quantized signal is then coded as a series of integers, $\Omega_L = \{w_1, w_2, ..., w_{n-L+1}\}$, where L is the length of consecutive sequence, $10 \leq L \leq 30$. Then the Shannon entropy of Ω_L is defined as follows:

$$SE(L) = \sum_{j=0}^{10^{L-1}} p_{\Omega_L}(j) \ln p_{\Omega_L}(j) \tag{3}$$

where $p_{\Omega_L}(j)$ represent the approximated sample probability of the value j in Ω_L. Using the approximated Shannon entropy, the normalized entropy rate can be computed as:

$$NER(L) = \frac{SE(L) - SE(L-1) + SE(1)perc(L)}{SE(1)} \tag{4}$$

where $perc(L)$ is the percentage of the integers in Ω_L that appeared only once. Then the regularity index ρ, which is the entropy rate in our study, can be computed as:

$$\rho = 1 - min(NER(L)) \tag{5}$$

The cross-entropy rate describes how accurately can one signal predict another signal (Porta et al., 2000). To get the expression of the cross-entropy rate, $\Lambda_{X|Y}$, we simply extended from the derivation of the entropy rate above, which yields the definition of the normalized cross-entropy of X given by Y as:

$$NER_{X|Y}(L) = \frac{SE(L) - SE_{X|Y}(L-1) + SE_Y(1)perc_{X|Y}(L)}{SE_X(1)} \tag{6}$$

where $perc_{X|Y}(L)$ is the percentage the integers in $\Omega_L^{X|Y}$ that appeared only once. Then the index of synchronization which is the cross-entropy rate $\Lambda_{X|Y}$ in our study, can be computed as

$$\Lambda_{X|Y} = 1 - min(UF_{X|Y}(L)) \tag{7}$$

where $UF_{X|Y}(L)$ is the uncoupling function defined as follows:

$$UF_{X|Y}(L) = min(NCER_{X|Y}(L), NCER_{Y|X}(L)) \tag{8}$$

3.3. Frequency features

Peak frequency (f_p), bandwidth (B) and spectral centroid (f_c) were introduced to identify characteristics of signals in the frequency domain. Peak frequency is defined as the frequency at the maximum spectral power, which is given by the following (Sejdić et al., 2010):

$$f_p = \text{argmax}_f \left\{ |F_X(f)|^2 \right\} \tag{9}$$

where F_X is the Fourier transform of the original signal. It measures the frequency value where the largest power occurs. The centroid frequency (f_c) indicating the center of mass of the spectrum is given by (Quan and Harris,

1997):

$$f_c = \frac{\int_0^{f_{max}} f|F_X(f)|^2 df}{\int_0^{f_{max}} |F_X(f)|^2 df} \tag{10}$$

The bandwidth (B) is defined as following (Li, 2000):

$$B = \sqrt{\frac{\int_0^{f_{max}} (f - f_c)^2 |F_X(f)|^2 df}{\int_0^{f_{max}} |F_X(f)|^2 df}} \tag{11}$$

3.4. Time-frequency features

The wavelet transform is used to analyze signals by decomposing complex time-frequency information into elementary forms at different positions and scales (Sifuzzaman et al., 2009), (Stanković et al., 2012). Based on the 10-level discrete wavelet decomposition of the signal calculated using the Meyer wavelet (Sejdić et al., 2009), the relative wavelet energy (RWE) and the wavelet entropy (WE) are defined by the following equations (Lee et al., 2010):

$$E_{a_{10}} = \frac{\|a_{10}\|^2}{\|a_{10}\|^2 + \sum_{k=1}^{10} \|d_k\|^2} \times 100 \tag{12}$$

$$E_{d_k} = \frac{\|d_k\|^2}{\|a_{10}\|^2 + \sum_{k=1}^{10} \|d_k\|^2} \times 100 \tag{13}$$

$$\Omega = -E_{a_{10}} \log_2 E_{a_{10}} - \sum_{k=1}^{10} \log_2 E_{d_k} \tag{14}$$

where a_{10} is the approximation coefficient and d_k is the k^th-level detail coefficient in the 10-level decomposition in the Meyer wavelet. $\|\|$ is the Euclidean norm. The relative wavelet energy depicts the relative energy contained

within different frequency bands in the CBFV data. WE measures the degree of time-frequency order/disorder of the signal (Rosso et al., 2001).

4. Results

Throughout the experiment, all 20 subjects were observed to maintain a steady rate of respiration and a stable $ETCO_2$ level (31.85 ± 3.59 mmHg). Hence, the effect of $ETCO_2$ on CBFV was not further considered. Calculations of different characteristics were applied to the specific testing period to reflect various features of signals in three phases: resting state, verbal tasks, and geometric tasks. The average values of these features are shown in this section within different groups based on feature type. p-values were calculated using the Wilcoxon rank-sum test to determine the statistical difference between tasks and genders. The subsections below summarize the differences in features throughout the resting state, verbal task, and geometric task, denoted by "R","V" and "G" in the tables.

4.1. Time features

Table 1 summarizes time-domain features for both raw and envelope signals. These tables establish a clear comparison between L-MCA and R-MCA. While considering the features based on raw CBFV signals, the statistical differences were observed between the geometric task and the rest period for L-MCA kurtosis ($p = 0.04$) and correlation values ($p < 0.01$). Differences were also observed between verbal tasks and geometric tasks in correlation values ($p < 0.01$). Furthermore, the correlation values were affected by sex when considering the raw CBFV signal in the verbal tasks, the geometric

tasks, and rest ($p \ll 0.01$). Males had a higher correlation value than females.

For envelope CBFV signals, geometric tasks had statistically higher values of the R-MCA standard deviation ($p = 0.04$). However, when considering the envelope CBFV signal, sex effects occurred in almost all the features, except for L-R correlation values for verbal and geometric tasks. Generally, females had a higher standard deviation while males had higher skewness and kurtosis values. Obviously, there are statistical differences between between CBFV signals and envelope CBFV signals when considering the time domain features ($p \ll 0.01$).

4.2. Information-theoretic features

Information-theoretic features from raw CBFV signals and envelope CBFV signals are shown in Table 2. When considering raw CBFV signals during different cognitive tasks, the synchronization index was statistically higher during the resting state than during the geometric task ($p = 0.03$). Verbal tasks had a lower LZC mean value than resting state and geometric tasks in both MCAs. There were also sex-based differences: males had statistically higher $\Lambda_{R|L}$ values than females for all kinds of tasks ($p < 0.01$). Additionally, males also had statistically higher values of LZC and ρ from R-MCA during rest ($p < 0.01$).

When considering the envelope CBFV signals during different cognitive tasks, statistical differences were observed between verbal tasks and the resting state in LZC on L-MCA, ρ on L-MCA, and $\Lambda_{R|L}$ ($p < 0.02$). Statistical differences between geometric tasks and the resting state were observed in all the features from both MCAs ($p < 0.04$). The resting state had a lower

LZC value and higher ρ and $\Lambda_{R|L}$ values on both sides. Sex effects were more pronounced when considering the envelope CBFV signals. Statistical differences were observed in all features from both sides ($p < 0.03$). Females had a higher LZC value while males had higher ρ and $\Lambda_{R|L}$ values.

Statistical differences were observed between raw CBFV signals and envelope CBFV signals in all features ($p < 0.02$) except that of LZC in R-MCA during verbal and geometric tasks.

4.3. Frequency features

Table 3 summarize frequency features for the raw and envelope signals, respectively. For the raw CBFV signals, statistical differences were observed between geometric tasks and rests in the spectral centroid for both left and right MCA ($p < 0.02$), and between geometric tasks and verbal tasks in the spectral centroid for R-MCA ($p = 0.02$). While considering the sex effects, we found that all features except the bandwidth values from L-MCA were statistically different for all cognitive tasks ($p < 0.01$). Frequency features of females were generally higher than those values for males.

When considering envelope CBFV signals, no statistical difference was found between cognitive tasks from either hemisphere. There were sex-based statistical differences observed for peak frequency values ($p < 0.01$) in all three tasks from both sides except that from L-MCA in geometric tasks. There was also a sex-based difference in spectral centroid values from R-MCA ($p < 0.01$).

Obviously, the raw signals had a higher frequency content than the envelope CBFV signals ($p \ll 0.01$).

4.4. Time-frequency features

Figure 3 summarizes the relative wavelet energy distributions for raw right and left MCA signals. Statistical differences between verbal tasks and rests occurred in the d_2 decomposition level in L-MCA ($p = 0.03$); between geometric tasks and rests occurred in a_{10}, d_1, d_2, and d_7 in L-MCA ($p < 0.02$), and d_4, d_5, d_7 in R-MCA ($p < 0.02$); and between verbal and geometric tasks occurred in d_4, d_5, d_7 in R-MCA ($p < 0.05$). The wavelet entropy ranged from 1.80 to 1.84, but it was not statistically different between blood vessels or amongst tasks.

The relative wavelet energy distribution for the envelope signals was predominately concentrated in the a_{10} region (more than 99%). Hence, we did not consider any other regions. The wavelet entropy was 0.07 for all tasks, but it was not statistically different between blood vessels or tasks.

Also, the energy concentrations for both types of CBFV signals were greatly affected by gender. We present these differences in Table 4.

5. Discussion

Our findings presented here can be summarized into three major observations. First, most features extracted from raw and envelope signals are statistically different. Second, the cognitive tasks had significant effects on the raw signal and the envelope signal. Third, sex effects were observed in every set of characteristics.

Most features extracted from raw and envelope signals in all three domains are statistically different. These features demonstrated that the raw signals were more symmetric, more concentrated and had a significantly

higher frequency content than the envelope signals. The raw signals from L-MCA and R-MCA are highly independent, but both raw CBFV signals and envelope signals have a similar predictability. This was interesting as the raw CBFV signals have a higher ρ value than the envelope signals, which means the raw signals are more discorded and random than the envelope signals. The raw signals also have higher $\Lambda_{R|L}$ values, which indicates that the raw signal from one channel can be more easily predicted given the opposite channel than the envelope signals. Higher frequency content of the raw signals implied that these signals are robust low-frequency physiological artifacts (e.g.(Lohmann et al., 2005)) which contaminate the envelope signals. Lastly, the envelope signals had a simple time-frequency structure than the raw signals, as demonstrated by the wavelet entropy values and the relative energy distributions for both groups.

Different cognitive tasks induced changes in cerebral blood flow as demonstrated by the extracted features from raw and envelope signals. Specifically, geometric tasks induced significant changes in some of the statistical features associated with raw signals. However, verbal tasks and rests had more similarity in the statistical domain since no statistical difference in any features was observed between the two. The information-theoretic features provided a greater discrimination between the tasks for both envelope and raw signals. Verbal tasks and resting state had statistical differences mainly in L-MCA, while geometric tasks and the resting state had differences in all features from both sides. Hence, cognitive tasks, especially geometric rotation, were highly distinguished from the baseline. Similarly, in the frequency domain, there was an obvious increase in peak frequency and spectral centroid dur-

ing the verbal and geometric tasks in comparison to the resting state for the raw signals. This finding implies a stronger blood flow during cognitive tasks. This is consistent with the previous experiments which indicated that there was a global increase in the flow velocity above baseline during the task performance (e.g., (Hartje et al., 1994), (Droste et al., 1989a)). The verbal tasks experienced a more obvious increase in L-MCA, while the geometric tasks exhibited a larger change in R-MCA. The dominance of L-MCA in verbal tasks and the dominance in R-MCA in spatial tasks have been established in previous studies (e.g., (Risberg et al., 1975), (Gur et al., 1982), (Gur et al., 1987), (Corballis and Sergent, 1989)). The left hemisphere was also highly engaged in mental rotation tasks. This finding appears to be consistent with the recent dispute on the specialization of the right hemisphere in the process of mental rotation and visualization. Some studies alleged that the left hemisphere plays an important role especially in the process of mental rotation (e.g., (Fischer and Pellegrino, 1988), (Farah, 1989)). Based on this information, raw signals would be very helpful when determining the dominance of hemisphere which was not displayed in the envelope signals. However, the frequency features for envelope CBFV signals exhibited no significant changes between cognitive tasks. For the verbal tasks, there was a slight increase in peak frequency from both sides, and a slight increase in bandwidth and central frequency values from R-MCA. Geometric tasks only increased the bandwidth values from R-MCA. Envelope signals did not provide as much information as raw signals in identifying cognitive tasks, as they only contain low-frequency components, thus useful information in a higher frequency band is lost. No statistical differences in any features were

found between verbal tasks and rest conditions, which is consistent with the above analysis.

Lastly, sex effects were observed in every set of characteristics. Previous studies have shown that females have significantly higher velocities than age-matched males (e.g., (Russo et al., 1986), (Vriens et al., 1989)). However, those differences could be identified as global difference which existed in a baseline period, but sex effects were not obvious between cognitive tasks. Two previous activation studies have also mentioned that they found no sex differences (e.g., (Droste et al., 1989b), (Harders et al., 1989)). Based on our analysis, we can see that the sex differences in CBFV signals were consistent throughout different cognitive tasks.

Raw and envelope signals provide complimentary information. From a clinical point view, resulting differences in signal characteristics enable us to study cerebral blood flow from different perspectives and gain deeper understanding about the effects of cognitive loads on the MCA flow. Such results can be then translated into other fields. For example, understanding the MCA flow during a cognitive load would be useful to understand the effects of cognitive loads on walking patterns in older adults. Similarly, the sex effects on the MCA flow can be important for understanding the effects of menopause on cerebral blood flow in older females.

5.1. Future work and limitations

The future work can be based on several directions. First, understanding the cognitive effects on cerebral blood flow through the anterior cerebral arteries represents a next logical step. Such results would enable us to move towards our next potential goal which is the utility of TCD record-

ings as control signals in brain-computer interfaces. If the development of brain-computer interfaces based on TCD is a desirable goal, one should also investigate the effects of various disabilities on cerebral blood flow during resting-state conditions and different cognitive tasks. Lastly, future publications should also focus on determining a reduced robust set of features which consistently and accurately differentiate between different cognitive task and rests.

A major potential limitation based on our results is the fact that there were observed sex differences for various features. If these differences persist in a larger population, it would imply that any TCD-based BCI would require gender-based machine learning algorithms. A second limitation of the current study is that we only considered two cognitive tasks. Future studies should investigate whether such task are suitable for clinical populations.

6. Conclusions

In this study, we observed different characteristics between raw CBFV signals and envelope CBFV signals. The raw signals tend to be more symmetric and stable, but more disordered than the envelope signals. The raw signals also had higher frequency, and the energy was distributed in high frequencies. The envelope signals' energy were concentrated in a low frequency region. We found that the raw CBFV signals provides valuable information when determining the effects of cognitive tasks and lateralization. These results showed that the raw CBFV signals provided different information from the envelope signal, which proved valuable in studying changes in cognitive tasks and lateralization in cerebral blood flow velocity. TCD shows poten-

tial in studying brain function. However, the current study only considered healthy participants. Hence, our future research will aim to investigate the considered features in patients with disabilities in order to understand differences in the extracted features and possibly work towards a TCD-based brain-machine interface.

Acknowledgements

The authors would like to express the greatest gratitude to all the participants.

References

Aaslid, R., Markwalder, T.-M., Nornes, H., 1982. Noninvasive transcranial Doppler ultrasound recording of flow velocity in basal cerebral arteries. Journal of Neurosurgery 57 (6), 769–774.

Aboy, M., Hornero, R., Abásolo, D., Álvarez, D., 2006. Interpretation of the Lempel-Ziv complexity measure in the context of biomedical signal analysis. IEEE Transactions on Biomedical Engineering 53 (11), 2282–2288.

Alexandrov, A. V., Sloan, M. A., Wong, L. K., Douville, C., Razumovsky, A. Y., Koroshetz, W. J., Kaps, M., Tegeler, C. H., 2007. Practice standards for transcranial Doppler ultrasound: Part i - test performance. Journal of Neuroimaging 17 (1), 11–18.

Corballis, M. C., Sergent, J., 1989. Mental rotation in a commissurotomized subject. Neuropsychologia 27 (5), 585–597.

Cover, T. M., Thomas, J. A., 2006. Elements of information theory. Wiley-interscience.

Deppe, M., Knecht, S., Papke, K., Lohmann, H., Fleischer, H., Heindel, W., Ringelstein, E. B., Henningsen, H., 2000. Assessment of hemispheric language lateralization: A comparison between fMRI and fTCD. Journal of Cerebral Blood Flow and Metabolism 20 (2), 263–268.

Deppe, M., Ringelstein, E. B., Knecht, S., 2004. The investigation of functional brain lateralization by transcranial doppler sonography. Neuroimage 21 (3), 1124–1146.

Diehl, R., Sitzer, M., Hennerici, M., 1990. Changes of cerebral blood flow velocity during cognitive activity. Stroke 21 (8), 1236–1237.

Droste, D. W., Harders, A. G., Rastogi, E., 1989a. A transcranial Doppler study of blood flow velocity in the middle cerebral arteries performed at rest and during mental activities. Stroke 20 (8), 1005–1011.

Droste, D. W., Harders, A. G., Rastogi, E., 1989b. Two transcranial Doppler studies on blood flow velocity in both middle cerebral arteries during rest and the performance of cognitive tasks. Neuropsychologia 27 (10), 1221–1230.

Duschek, S., Schandry, R., 2003. Functional transcranial doppler sonography as a tool in psychophysiological research. Psychophysiology 40 (3), 436–454.

Farah, M. J., 1989. The neural basis of mental imagery. Trends in Neurosciences 12 (10), 395–399.

Fischer, S. C., Pellegrino, J. W., 1988. Hemisphere differences for components of mental rotation. Brain and Cognition 7 (1), 1–15.

Gur, R. C., Gur, R. E., Obrist, W. D., Hungerbuhler, J. P., Younkin, D., Rosen, A. D., Skolnick, B. E., Reivich, M., Aug. 1982. Sex and handedness differences in cerebral blood flow during rest and cognitive activity. Science 217 (4560), 659–661.

Gur, R. C., Gur, R. E., Obrist, W. D., Skolnick, B. E., Reivich, M., 1987. Age and regional cerebral blood flow at rest and during cognitive activity. Archives of General Psychiatry 44 (7), 617.

Gur, R. C., Reivich, M., 1980. Cognitive task effects on hemispheric blood flow in humans: Evidence for individual differences in hemispheric activation. Brain and Language 9 (1), 78–92.

Harders, A., Laborde, G., Droste, D., Rastogi, E., 1989. Brain activity and blood flow velocity changes: a transcranial Doppler study. International Journal of Neuroscience 47 (1-2), 91–102.

Hartje, W., Ringelstein, E. B., Kistinger, B., Fabianek, D., Willmes, K., 1994. Transcranial Doppler ultrasonic assessment of middle cerebral artery blood flow velocity changes during verbal and visuospatial cognitive tasks. Neuropsychologia 32 (12), 1443–1452.

Huber, P., Handa, J., 1967. Effect of contrast material, hypercapnia, hyperventilation, hypertonic glucose and papaverine on the diameter of the cerebral arteries: angiographic determination in man. Investigative Radiology 2 (1), 17–32.

Ingvar, D., Risberg, J., 1965. Influence of mental activity upon regional cerebral blood flow in man. Acta Neurologica Scandinavica 41 (S14), 183–186.

Kelley, R., Chang, J., Scheinman, N., Levin, B., Duncan, R., Lee, S.-C., 1992. Transcranial Doppler assessment of cerebral flow velocity during cognitive tasks. Stroke 23 (1), 9–14.

Klingelhöfer, J., Matzander, G., Sander, D., Conrad, B., 1994. Bilateral changes of middle cerebral artery blood flow velocities in various hemisphere-specific brain activities. Journal of Neurology 241, 264–265.

Klingelhöfer, J., Matzander, G., Sander, D., Schwarze, J., Boecker, H., Bischoff, C., 1997. Assessment of functional hemispheric asymmetry by bilateral simultaneous cerebral blood flow velocity monitoring. Journal of Cerebral Blood Flow and Metabolism 17 (5), 577–585.

Knecht, S., Deppe, M., Ebner, A., Henningsen, H., Huber, T., Jokeit, H., Ringelstein, E.-B., 1998a. Noninvasive determination of language lateralization by functional transcranial Doppler sonography a comparison with the Wada test. Stroke 29 (1), 82–86.

Knecht, S., Deppe, M., Ringelstein, E.-B., Wirtz, M., Lohmann, H., Dräger, B., Huber, T., Henningsen, H., 1998b. Reproducibility of functional transcranial Doppler sonography in determining hemispheric language lateralization. Stroke 29 (6), 1155–1159.

Lassen, N. A., Ingvar, D. H., Skinhoj, E., 1978. Brain function and blood flow. Scientific American 239 (4), 62–71.

Lee, J., Sejdić, E., Steele, C. M., Chau, T., et al., 2010. Effects of liquid stimuli on dual-axis swallowing accelerometry signals in a healthy population. Biomedical Engineering Online 9 (1), 7.

Lempel, A., Ziv, J., 1976. On the complexity of finite sequences. IEEE Transactions on Information Theory 22 (1), 75–81.

Li, S. Z., 2000. Content-based audio classification and retrieval using the nearest feature line method. IEEE Transactions on Speech and Audio Processing 8 (5), 619–625.

Lohmann, H., Dräger, B., Müller-Ehrenberg, S., Deppe, M., Knecht, S., 2005. Language lateralization in young children assessed by functional transcranial Doppler sonography. Neuroimage 24 (3), 780–790.

Markus, H., Boland, M., 1992. Cognitive activity monitored by non-invasive measurement of cerebral blood flow velocity and its application to the investigation of cerebral dominance. Cortex.

Markwalder, T.-M., Grolimund, P., Seiler, R. W., Roth, F., Aaslid, R., 1984. Dependency of blood flow velocity in the middle cerebral artery on end-tidal carbon dioxide partial pressure: a transcranial ultrasound Doppler study. Journal of Cerebral Blood Flow and Metabolism 4 (3), 368–372.

Matteis, M., Bivona, U., Catani, S., Pasqualetti, P., Formisano, R., Vernieri, F., Troisi, E., Caltagirone, C., Silvestrini, M., 2009. Functional transcranial Doppler assessment of cerebral blood flow velocities changes during attention tasks. European Journal of Neurology 16 (1), 81–87.

Monsein, L. H., Razumovsky, A. Y., Ackerman, S. J., Nauta, H. J., Hanley, D. F., 1995. Validation of transcranial Doppler ultrasound with a stereotactic neurosurgical technique. Journal of Neurosurgery 82 (6), 972–975.

Myrden, A., Kushki, A., Sejdić, E., Chau, T., Oct. 2012. Towards increased data transmission rate for a three-class metabolic brain-computer interface based on transcranial Doppler ultrasound. Neuroscience Letters 528 (2), 99–103.

Myrden, A. J. B., Kushki, A., Sejdić, E., Guerguerian, A.-M., Chau, T., Sep. 2011. A brain-computer interface based on bilateral transcranial Doppler ultrasound. PLoS ONE 6 (9), e24170–1–8.

Oldfield, R. C., 1971. The assessment and analysis of handedness: the edinburgh inventory. Neuropsychologia 9 (1), 97–113.

Papoulis, A., 1991. Probability, Random Variables, and Stochastic Processes, 3rd Edition. WCB/McGraw-Hill, New York.

Paulson, O. B., Hasselbalch, S. G., Rostrup, E., Knudsen, G. M., Pelligrino, D., 2009. Cerebral blood flow response to functional activation. Journal of Cerebral Blood Flow and Metabolism 30 (1), 2–14.

Peters, M., Battista, C., 2008. Applications of mental rotation figures of the Shepard and Metzler type and description of a mental rotation stimulus library. Brain and Cognition 66 (3), 260–264.

Porta, A., Guzzetti, S., Montano, N., Furlan, R., Pagani, M., Malliani, A., Cerutti, S., 2001. Entropy, entropy rate, and pattern classification as tools

to typify complexity in short heart period variability series. IEEE Transactions on Biomedical Engineering 48 (11), 1282–1291.

Porta, A., Guzzetti, S., Montano, N., Pagani, M., Somers, V., Malliani, A., Baselli, G., Cerutti, S., 2000. Information domain analysis of cardiovascular variability signals: evaluation of regularity, synchronisation and co-ordination. Medical and Biological Engineering and Computing 38 (2), 180–188.

Quan, Y., Harris, J. M., 1997. Seismic attenuation tomography using the frequency shift method. Geophysics 62 (3), 895–905.

Risberg, J., 1986. Regional cerebral blood flow in neuropsychology. Neuropsychologia 24 (1), 135–140.

Risberg, J., Halsey, J. H., Wills, E. L., Wilson, E. M., 1975. Hemispheric specialization in normal man studied by bilateral measurements of the regional cerebral blood flow a study with the 133-xe inhalation technique. Brain 98 (3), 511–524.

Risberg, J., Ingvar, D. H., 1973. Patterns of activation in the grey matter of the dominant hemisphere during memorizing and reasoning. a study of regional cerebral blood flow changes during psychological testing in a group of neurologically normal patients. Brain 96 (4), 737–756.

Rosso, O. A., Blanco, S., Yordanova, J., Kolev, V., Figliola, A., Schurmann, M., Basar, E., 2001. Wavelet entropy: a new tool for analysis of short duration brain electrical signals. Journal of Neuroscience Methods 105 (1), 65–76.

Russo, G., Profeta, G., Acampora, S., Troisi, F., 1986. Transcranial Doppler ultrasound: examination technique and normal reference values. Journal of the Neurological Sciences 30, 97–102.

Schmidt, P., Krings, T., Willmes, K., Roessler, F., Reul, J., Thron, A., 1999. Determination of cognitive hemispheric lateralization by functional transcranial Doppler cross-validated by functional MRI. Stroke 30 (5), 939–945.

Sejdić, E., Djurović, I., Jiang, J., 2009. Time-frequency feature representation using energy concentration: An overview of recent advances. Digital Signal Processing 19 (1), 153–183.

Sejdić, E., Kalika, D., Czarnek, N., 2013. An analysis of resting-state functional transcranial Doppler recordings from middle cerebral arteries. PloS ONE 8 (2), e55405–1–9.

Sejdić, E., Steele, C., Chau, T., Oct. 2010. The effects of head movement on dual-axis cervical accelerometry signals. BMC Research Notes 3 (1), 269–1–6.

Sifuzzaman, M., Islam, M. R., Ali, M. Z., 2009. Application of wavelet transform and its advantages compared to Fourier transform. Journal of Physical Sciences 13, 121–134.

Silvestrini, M., Cupini, L. M., Matteis, M., Troisi, E., Caltagirone, C., 1994. Bilateral simultaneous assessment of cerebral flow velocity during mental activity. Journal of Cerebral Blood Flow and Metabolism 14 (4), 643–648.

Stanković, S., Orović, I., Sejdić, E., 2012. Multimedia Signals and Systems. Springer US, New York, NY.

Stroobant, N., Vingerhoets, G., 2000. Transcranial Doppler ultrasonography monitoring of cerebral hemodynamics during performance of cognitive tasks: a review. Neuropsychology Review 10 (4), 213–231.

Tiecks, F. P., Haberl, R. L., Newell, D. W., 1998. Temporal patterns of evoked cerebral blood flow during reading. Journal of Cerebral Blood Flow and Metabolism 18 (7), 735–741.

Vriens, E., Kraaier, V., Musbach, M., Wieneke, G., Van Huffelen, A., 1989. Transcranial pulsed Doppler measurements of blood velocity in the middle cerebral artery: reference values at rest and during hyperventilation in healthy volunteers in relation to age and sex. Ultrasound in Medicine and Biology 15 (1), 1–8.

White, H., Venkatesh, B., 2006. Applications of transcranial Doppler in the ICU: a review. Intensive Care Medicine 32 (7), 981–994.

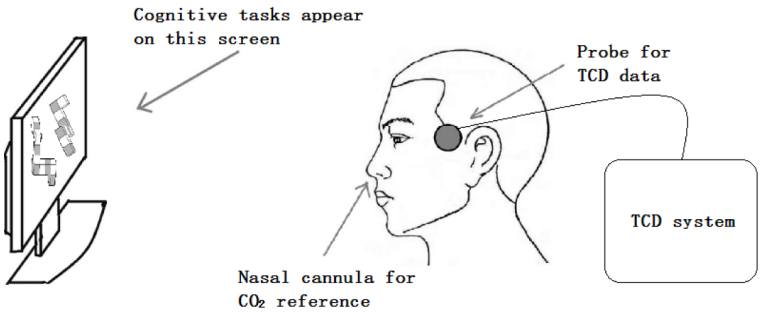

Figure 1: Setup for the TCD experiment: a cognitive task is displayed on a screen, while TCD probes are placed on transtemporal windows and a nasal cannula is placed over the nose.

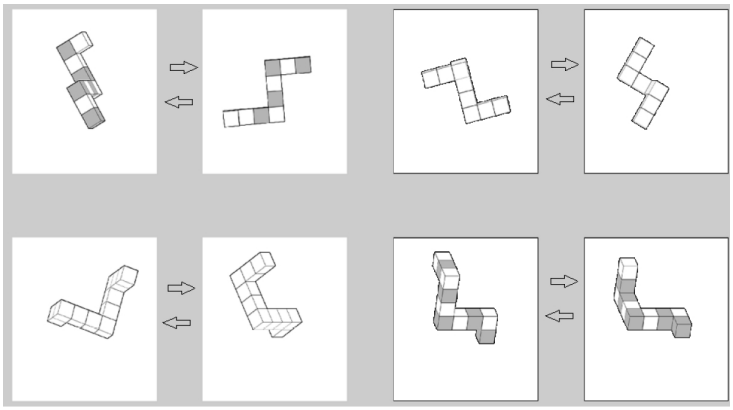

Figure 2: A sample of the on-screen geometric task. The users were instructed to decide whether the pair of geometric patterns were identical by mentally rotating them. This figure shows four pairs.

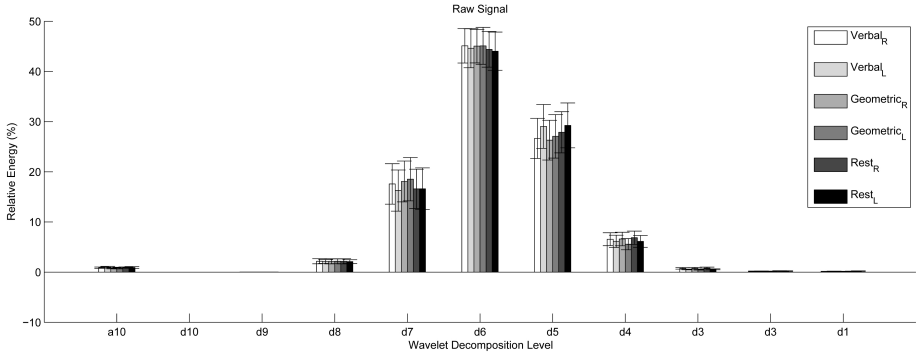

Figure 3: A sample of the on-screen geometric task. The users were instructed to mentally tell whether the pair of geometric patterns were identical by mentally rotating them. This figure shows four pairs.

Table 1: Time features from raw (denoted by the subscript r) and envelope (denoted by the subscript e) CBFV signals. * denotes multiplication by 10^{-4}; † denotes statistical differences between R and G; ‡ denotes statistical differences between V and G.

Raw	Standard Deviation (σ)		Skewness (ξ)		Kurtosis (γ)		Correlation L-R
	L-MCA	R-MCA	L-MCA	R-MCA	L-MCA	R-MCA	
R_r	0.23±0.14	0.22±0.14	(-1.87±30.19)*	(-1.34±24.37)*	2.99±0.36†	3.01±0.40	0.012±0.001†
V_r	0.23±0.14	0.22±0.14	(-0.96±23.21)*	(1.99±19.07)*	2.97±0.35	2.97±0.37	0.012±0.001‡
G_r	0.24±0.14	0.22±0.14	(-1.76±25.17)*	(-0.67±17.11)*	2.96±0.35†	2.96±0.38	0.012±0.001†‡
R_e	12.5±2.83	12.3±2.56	0.87±0.32	0.90±0.38	3.85±0.81	3.94±1.26	0.98±0.01
V_e	12.5±2.73‡	12.3±2.56	0.87±0.32	0.90±0.38	3.85±0.81	3.94±1.26	0.98±0.01
G_e	12.6±2.78‡	12.4±2.61	0.85±0.31	0.86±0.36	3.70±0.73	3.77±1.11	0.98±0.01

Table 2: Information-theoretic features from raw (denoted by the subscript r) and envelope (denoted by the subscript e) CBFV signals. † denotes statistical differences between R and G; ‡ denotes statistical differences between V and G; § denotes statistical differences between V and G.

Raw	Lempel-Ziv complexity (LZC)		Entropy rate (ρ)		Synchronization index ($\Lambda_{R\|L}$)
	L-MCA	R-MCA	L-MCA	R-MCA	
R_r	$0.67\pm0.08^{\S}$	$0.66\pm0.08^{\S}$	0.68 ± 0.20	0.70 ± 0.16	$0.72\pm0.16^{\dagger}$
V_r	$0.65\pm0.12^{\ddagger\S}$	$0.64\pm0.12^{\ddagger\S}$	0.68 ± 0.21	0.70 ± 0.17	0.72 ± 0.17
G_r	$0.67\pm0.09^{\ddagger}$	$0.66\pm0.09^{\ddagger}$	0.66 ± 0.20	0.69 ± 0.16	$0.70\pm0.16^{\dagger}$
R_e	$0.66\pm0.03^{\dagger}$	$0.66\pm0.03^{\dagger\S}$	$0.28\pm0.16^{\dagger}$	$0.28\pm0.15^{\dagger}$	$0.33\pm0.15^{\dagger\S}$
V_e	0.67 ± 0.03	$0.66\pm0.03^{\S}$	0.23 ± 0.14	0.26 ± 0.14	$0.30\pm0.13^{\S}$
G_e	$0.67\pm0.02^{\dagger}$	$0.66\pm0.04^{\dagger}$	$0.23\pm0.14^{\dagger}$	$0.25\pm0.15^{\dagger}$	$0.29\pm0.13^{\dagger}$

Table 3: Frequency features from raw (denoted by the subscript r) and envelope (denoted by the subscript e) CBFV signals. † denotes statistical differences between R and G; ‡ denotes statistical differences between V and G. The values are in the SI unit Hz.

Raw	Peak Frequency (f_p)		Bandwidth (B)		Spectral Centroid (f_c)	
	L-MCA	R-MCA	L-MCA	R-MCA	L-MCA	R-MCA
R_r	784±258	776±309	547±98.2	534±85.9	973±208†	970±225†
V_r	804±273	779±316	548±96.9	534±85.6	992±211	969±220‡
G_r	815±281	824±303	548±96.5	536±82.0	998±213†	1006±234†‡
R_e	1.16±0.52	1.16±0.50	10.02±2.78	9.22±2.27	7.47±3.45	6.23±2.31
V_e	1.21±0.52	1.21±0.50	10.01±2.77	9.34±2.27	7.47±3.44	6.39±2.35
G_e	1.16±0.46	1.18±0.49	10.06±2.77	9.23±2.25	7.54±3.56	6.20±2.36

Table 4: Sex effects one time-frequency features from raw (denoted by the subscript r) and envelope (denoted by the subscript e) CBFV signals. $\surd$ denotes a statistical difference.

	Rest Period		Verbal Task		Geometric Task	
	L-MCA	R-MCA	L-MCA	R-MCA	L-MCA	R-MCA
Ω_r						
$E_{r_{a_{10}}}$		$\surd$		$\surd$		$\surd$
$E_{r_{d_{10}}}$	$\surd$				$\surd$	
$E_{r_{d_9}}$	$\surd$		$\surd$		$\surd$	
$E_{r_{d_8}}$		$\surd$		$\surd$		$\surd$
$E_{r_{d_7}}$	$\surd$	$\surd$	$\surd$	$\surd$	$\surd$	$\surd$
$E_{r_{d_6}}$	$\surd$	$\surd$		$\surd$		$\surd$
$E_{r_{d_5}}$	$\surd$	$\surd$	$\surd$	$\surd$	$\surd$	$\surd$
$E_{r_{d_4}}$	$\surd$	$\surd$	$\surd$	$\surd$		$\surd$
$E_{r_{d_3}}$	$\surd$	$\surd$	$\surd$	$\surd$	$\surd$	$\surd$
$E_{r_{d_2}}$	$\surd$		$\surd$	$\surd$	$\surd$	$\surd$
$E_{r_{d_1}}$	$\surd$	$\surd$	$\surd$	$\surd$	$\surd$	$\surd$
Ω_e	$\surd$	$\surd$	$\surd$	$\surd$	$\surd$	$\surd$
$E_{e_{a_{10}}}$	$\surd$	$\surd$	$\surd$	$\surd$	$\surd$	$\surd$